Laminar Flow around an Array of 3D Protruding Heaters Mounted in Cross-Stream Direction

By Felipe Baptista Nishida & Thiago Antonini Alves

Universidade Tecnológica Federal do Paraná (UTFPR), Brazil

Abstract- Numerical analysis was performed to investigate the characteristics of the laminar fluid flow around an array of 3D protruding heaters mounted on the bottom substrate of a parallel plane channel using the ANSYS/Fluent® 14.0 commercial software. The fluid flow was considered to have constant properties under steady state conditions. In the channel inlet, the velocity profile was uniform. This problem is associated with forced flow over the electronic components mounted on printed circuit boards. The conservation equations and their boundary conditions were numerically solved in a single domain through a coupled procedure. The discretization of the equations was based on the Control Volumes Method. The algorithm SIMPLE was used to solve the pressure-velocity couple. Due to the non-linearity of the momentum equation, the correction of the velocity components and the pressure were under-relaxed to prevent instability and divergence. After a study of the computational mesh independence, the numerical results were obtained, displayed as a 3D non-uniform mesh with 212,670 control volumes. This computational mesh was more concentrated near the solid-fluid interface regions due to the larger primitive variable gradients in these regions. An investigation was done on the effects of the Reynolds numbers where the Reynolds numbers ranged from 100 to 300 and was dependent on the heights of the protruding heaters. The main characteristics of the fluid flow consisted of a small recirculation upstream of the heaters, the formation of horseshoe vortices around the protruding heaters' side walls and a large recirculation region downstream of the heaters.

Keywords: laminar flow, 3D protruding heaters, streamlines, recirculation, horseshoe vortices.

GJRE-A Classification : FOR Code: 091399p

LAMINARFLOWAROUNDANARRAYOF3DPROTRUDINGHEATERSMOUNTEDINCROSSSTREAMDIRECTION

Strictly as per the compliance and regulations of:

Laminar Flow around an Array of 3D Protruding Heaters Mounted in Cross-Stream Direction

Felipe Baptista Nishida [α] & Thiago Antonini Alves[σ]

Abstract- Numerical analysis was performed to investigate the characteristics of the laminar fluid flow around an array of 3D protruding heaters mounted on the bottom substrate of a parallel plane channel using the ANSYS/Fluent® 14.0 commercial software. The fluid flow was considered to have constant properties under steady state conditions. In the channel inlet, the velocity profile was uniform. This problem is associated with forced flow over the electronic components mounted on printed circuit boards. The conservation equations and their boundary conditions were numerically solved in a single domain through a coupled procedure. The discretization of the equations was based on the Control Volumes Method. The algorithm SIMPLE was used to solve the pressure-velocity couple. Due to the non-linearity of the momentum equation, the correction of the velocity components and the pressure were under-relaxed to prevent instability and divergence. After a study of the computational mesh independence, the numerical results were obtained, displayed as a 3D non-uniform mesh with 212,670 control volumes. This computational mesh was more concentrated near the solid-fluid interface regions due to the larger primitive variable gradients in these regions. An investigation was done on the effects of the Reynolds numbers where the Reynolds numbers ranged from 100 to 300 and was dependent on the heights of the protruding heaters. The main characteristics of the fluid flow consisted of a small recirculation upstream of the heaters, the formation of horseshoe vortices around the protruding heaters' side walls and a large recirculation region downstream of the heaters. The fluid dynamics parameters of interest, the velocity profiles, local and average skin friction coefficient, pressure distribution and the Darcy-Weisbach friction factor, were found and compared to the results available in the literature.

Keywords: laminar flow, 3D protruding heaters, streamlines, recirculation, horseshoe vortices.

I. Introduction

The search for improvements and technological innovations by means of industrial development and academic research on the cooling of electronic equipment in the last two decades has been very intense. The most common method of heat transfer in source elements is still convection cooling, utilizing air as the work fluid. This choice was made because air is easily available, the devices required to move it are normally low cost, and it is 100% non-polluting (Nishida, 2012). In this work, problems motivated by the Level 2 of electronic packaging, associated with the thermal

control of one row of 3D protruding heaters mounted on a printed circuit board (PCB) were considered, as shown in Fig. 1 (Alves, 2010). The available space for the heaters can be limited and the cooling process must be done through forced convection with moderate velocities (low *Reynolds* number) due to operational limitations and noise reduction. Under such conditions, there may not be enough space to work with heat sinks in these concentrate heat dissipation components. These components can be simulated by protruding blocks mounted on a parallel plate channel.
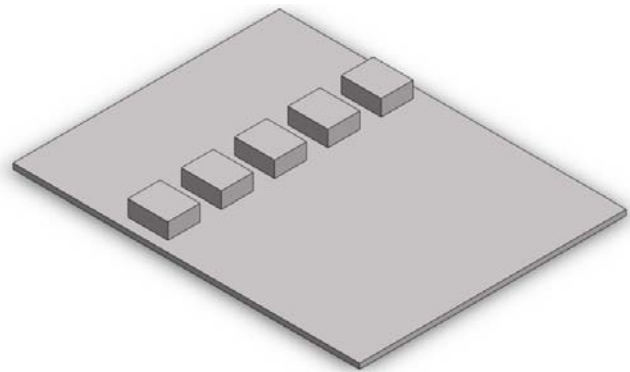
Figure 1 : Configuration of one row of 3D protruding heaters mounted on a PCB

Hwang & Yang (2004) presented a numerical study of the vortices structures of the flow (in a range of *Reynolds* numbers from low to moderate) around a cubic obstacle mounted on a plate in a channel. The main characteristics of the flow were horseshoe vortices upstream the obstacle, side vortices around the side faces of the cube, and "hair pin" vortices near the wake region. It was observed that as the flow approached the cube, an adverse pressure gradient produced a separate 3D boundary layer, allowing laminar horseshoe vortices to form. It was also noticed that as the *Reynolds* number increased, the structure of the horseshoe system became more complex and the number of vortices increased in pairs. Van Dijk& De Lange (2007) conducted a numerical study of a flow over one cubic obstacle mounted on the base of a parallel plate channel, considering either compressible or incompressible laminar flow. The *Reynolds* number was investigated in a range from 50 to 250, and the *Mach* number was varied between 0.1 and 0.6. The main flow characteristics around the obstacle were the formation of horseshoe vortices, vortices developing on the side

Authors α σ: DepartamentoAcadêmico de Mecânica (DAMEC), UniversidadeTecnológica Federal do Paraná (UTFPR), Campus Ponta Grossa, CEP 84.016-210, Ponta Grossa/PR, Brasil.
e-mails: felipenishida@hotmail.com, thiagoaalves@utfpr.edu.br

walls of the obstacle, and, downstream of the obstacle there was a wake with two counter-rotating vortices. It was noticed that the shape and size of these flow characteristics are determined mainly by the Reynolds number, verifying that for greater *Reynolds* numbers, the horseshoe vortices as well as the wake region extended over a significantly broader area. The correlation between the separation and reattachment point position with the *Reynolds* number was also presented. Other studies relating to the flow around 3D protruding heater(s) were performed by Castro & Robins (1977), Tropea&Gacktatter (1985), Martinuzzi&Tropea (1993), Okamoto*et al.* (1997).

II. ANALYSIS

The basic configuration representing the treated problem for one of the 3D protruding heaters is indicated

in Fig. 2. In this case, the channel has a height, H, length, L, and width, W. The substrate has the same length and width as the channel with a thickness, t. The heater has a length, L_h, height, H_h, width, W_h and it is located at a distance, L_u, from the channel entry. The space between the heaters is $2Ws$. The cooling process occurred through a forced laminar flow with constant properties under steady state conditions. In the channel entrance, the flow velocity profile (u_0) was considered uniform.

Figure 2 : Basic configuration representing the problem for one of the 3D protruding heaters

a) Problem Formulation

The mathematical model of the present problem was performed for a single domain: the solid regions (protruding heater and substrate) and the fluid flow in the channel. Due to the problem symmetries, the conservation equations were formulated for the domain with length, L, width, $W/2$ and height, $(H + t)$, as Fig. 3 shows.
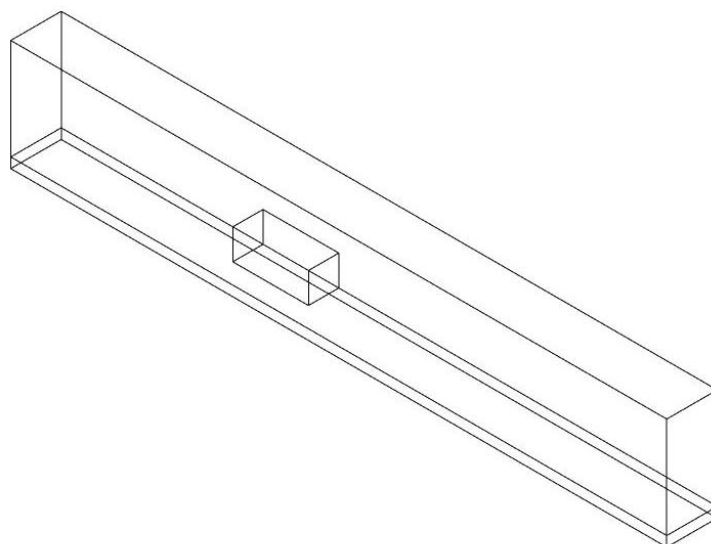
Figure 3 : Domain of the mathematical model analyzed

The governing equations cover the conservation principles in the considered domain. Steady state conditions, constant properties and negligible viscous dissipation were assumed. The occasional effects of oscillation in the flow are not being considered in this modeling: a typical procedure adopted in similar problems, i.e. Alves&Altemani (2012), Zeng &Vafai (2009) e Davalath&Bayazitoglu (1987).

- Mass Conservation *(Continuity Equation)*

$$\nabla \cdot \boldsymbol{u} = 0 \qquad (1)$$

- Momentum Conservation (Navier-Stokes Equation)

$$\rho(\boldsymbol{u} \cdot \nabla)\boldsymbol{u} = -\nabla p + \mu \nabla^2 \boldsymbol{u} \qquad (2)$$

The boundary conditions of the flow were uniform velocity (u_0) at the channel inlet, and null velocity at the solid-fluid interfaces (no-slip condition). At the channel outlet, the flow had its diffusion neglected in the *x* direction. In the solution domain at the lateral boundaries, the symmetry condition (periodic condition) was applied for the velocity fields (same geometry in each of the 3D protruding heater).

b) *Fluidynamic Parameters of Interest*

The solution of the governing equations output the velocity and pressure distributions in the considered domain. The numerical solutions of the primary variables distribution (*u, v, w, p*) were utilized to define the derived quantities. The *Reynolds* number in the channel was based on the protruding heater height (H_h) and calculated as

$$Re = \frac{\rho u_0 H_h}{\mu} = \frac{u_0 H_h}{\upsilon}. \qquad (3)$$

The local skin friction coefficient, $C_f(\xi)$, can be written as

$$C_f(\xi) = \frac{\tau_p(\xi)}{\left(\dfrac{\rho u_0^2}{2}\right)}. \qquad (4)$$

$\tau_p(\xi)$ is the local sheer stress in a surface of the heater.

The mean friction coefficient, $\overline{C}_f$, can be written as

$$\overline{C}_f = \frac{\overline{\tau}_p}{\left(\dfrac{\rho u_0^2}{2}\right)} \qquad . (5)$$

$\overline{\tau}_p$ iis the mean shear stress at the heater surfaces.

The *Darcy-Weisbach* (or *Moody*) friction factor can be defined in terms of the total pressure drop in the channel (*Δp*) by the equation

$$f = \frac{\Delta p \, H}{\left(\dfrac{\rho u_0^2}{2}\right)} \qquad (6)$$

c) *Numerical Solution*

The governing equations and their boundary conditions were numerically solved utilizing the Control Volume Method (Patankar, 1980) through the commercial software *ANSYS/Fluent*®14.0. The algorithm *SIMPLE (Semi-Implicit Method for Pressure Linked Equations)* was used to treat the pressure-velocity couple. The boundary conditions were applied at the edges of the analyzed domain (Fig. 3). After a mesh independency study, the numerical results were

obtained with a non-uniform 3D mesh containing 212,670 control volumes. This mesh was more concentrated in the regions near the solid-fluid interfaces due to the larger gradients in the primitive variables of these regions, as shown in Fig. 4. Due to the non-linearity in the *Momentum* Equation, the velocity components and the pressure correction were under-relaxed to prevent instability and divergence. The stop criteria of the iterative solving process was established for absolute changes in the primitive variables smaller than four significant figures between two consecutive iterations, while the global mass conservation in the domain was satisfied in all of the iterations. The numerical solutions were processed in a microcomputer with an *Intel®Core*™ 2 *Duo* E7500 2,94GHz processor and 4GB of RAM. The processing time of a typical solution was approximately 10 minutes.
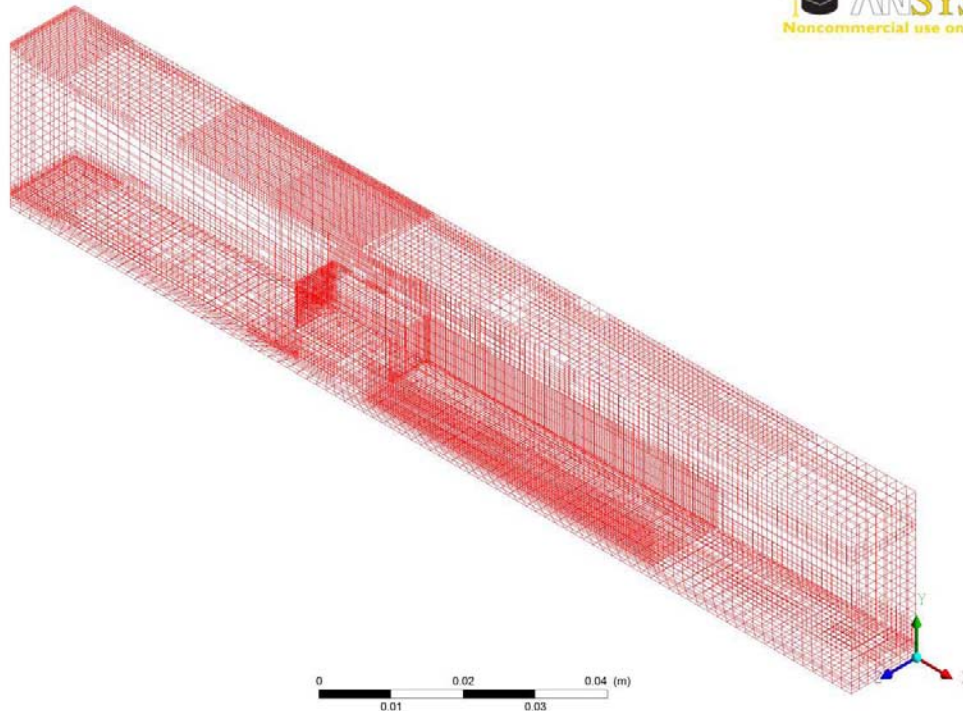
Figure 4 : 3D non-uniform mesh (3D perspective view)

III. Results and Discussion

Typical geometry and property values, relevant to the electronic components mounted on printed circuit board cooling applications, were used to obtain the numerical results (BAR-COHEN *et al.*, 2003). The geometric configuration showed in Fig. 2, were assumed considering a space $H = 0.0254$m between the parallel plates. Air was considered the cooling fluid. The fluid properties were considered constant, obtained at 300 K (INCROPERA *et al.*, 2008). The effects of the *Reynolds* numbers *Re* = 100, 150, 200, 250, and 300 were investigated. According to Morris &Garimella (1996), the flow is laminar for this range of *Re*.

In Figure 5, the streamlines over a 3D protruding heater, in a perspective view, are presented for *Reynolds* numbers of 100, 200, and 300. The main characteristics of the laminar flow are the horseshoe vortices which start upstream the heater and develop around the heater's lateral surfaces; a small recirculation upstream the protruding heater; the detachment of the fluid's boundary layer at the top of the heater causing a recirculation (reverse flux); and a large recirculation region downstream the heater due to the flow reattachment. It is interesting to state that the fluid flow development around the 3D protruding heaters' lateral surfaces does not freely happen due to the small space between the heaters.

(a)   Re = 100

(b)   Re = 200

(c)   Re = 300
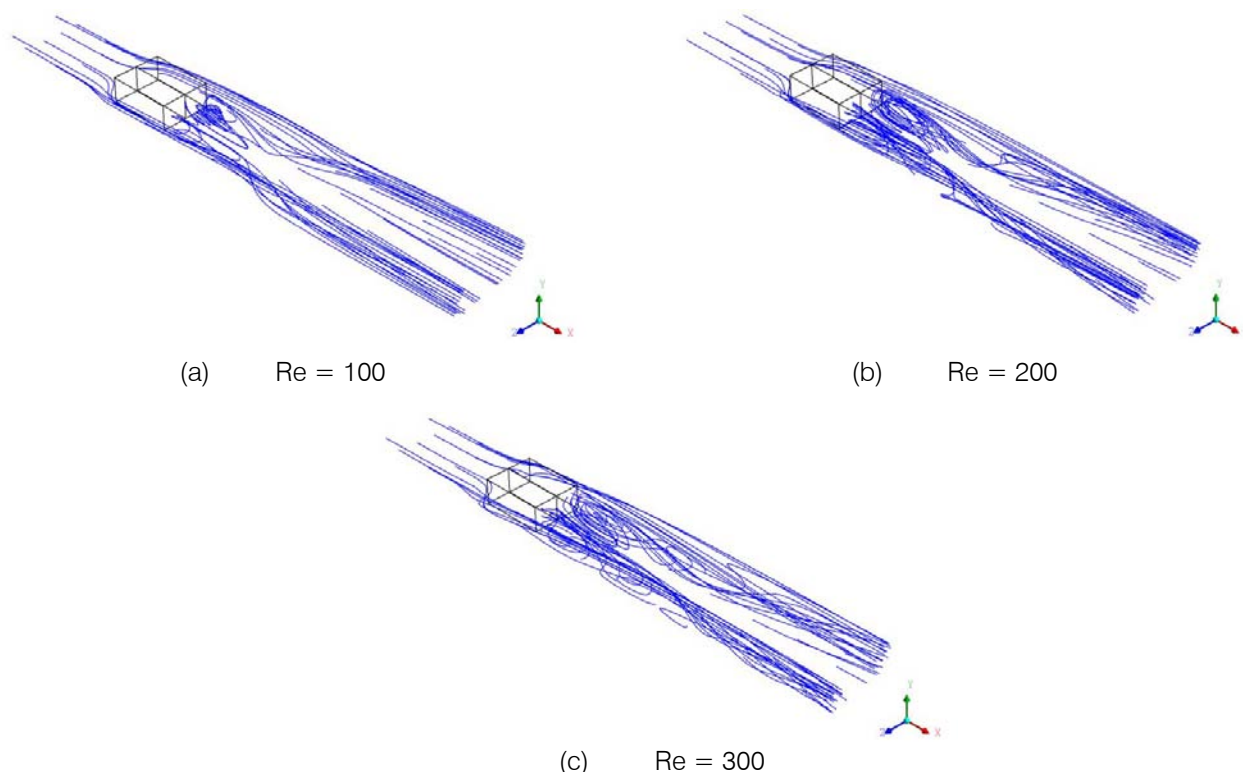
Figure 5 : Streamlines over a protruding heater (perspective 3D view)

In Figures 6, 7, and 8, streamlines are presented for the planes *xy, xz* e *yz*, respectively, for different *Reynolds* numbers. The characteristics of the flow over a 3D protruding heater can be better observed.

In Figure 6, as earlier mentioned, it can be observed a small recirculation upstream the heater, a detachment of the fluid boundary layer at the top of the heater making a recirculation (reverse flux), and a large recirculation downstream the heater due to the flow reattachment.

(a) Re = 100

(b) Re = 200

(c) Re = 300
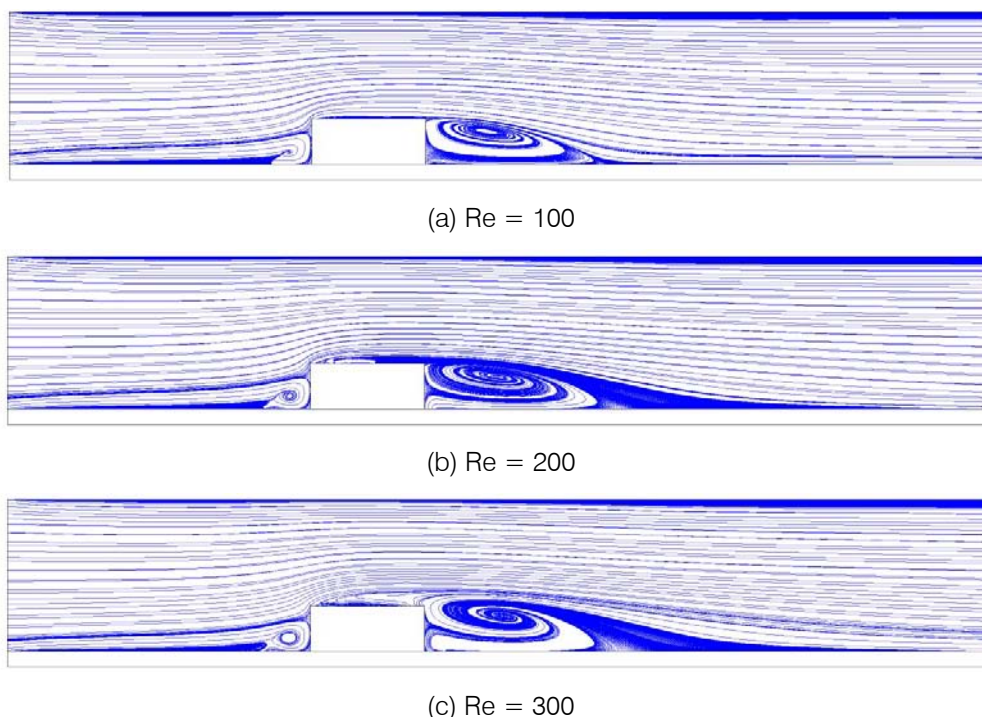
Figure 6 : Streamlines over a protruding heater on the plane xy for z = 0

In Figure 7, it is observed that the behavior of the streamlines downstream the recirculation region of a protruding heater becomes more complex when the *Reynolds* number is increased. It is also noticed that the recirculation length increases with the *Re*, in other words, the reattachment point of the fluid boundary layer gets further downstream the heater. It is emphasized that the fluid flow development around the 3D protruding heaters' lateral surfaces does not freely happen due to the small space between the heaters.

(a) Re = 100

(b) Re = 200

(c) Re = 300
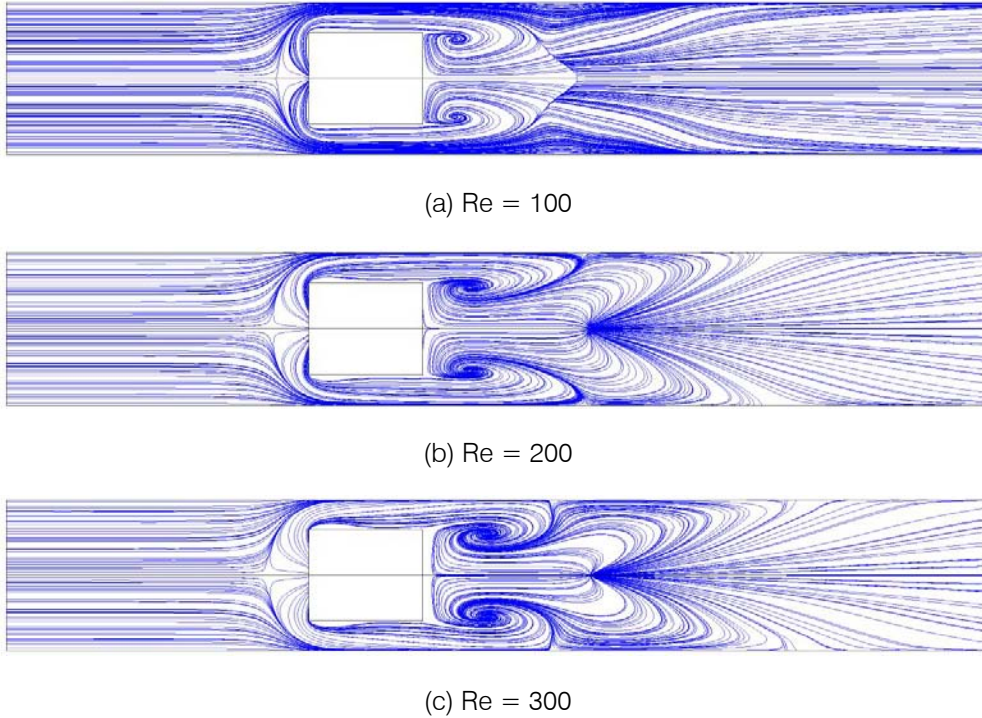
Figure 7 : Streamlines over a protruding heater on the plane xz for y = 0,16H

In Figure 8, it is seen that the laminar flow complexity over the protruding heater is greater with a larger *Reynolds* number.

(a) Re = 100

(a) Re = 200

(a) Re = 300
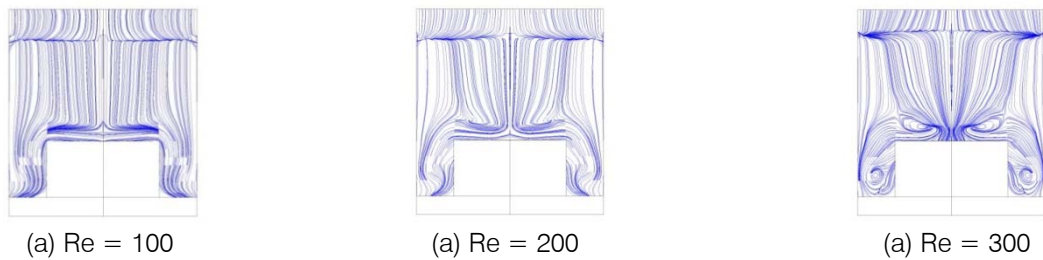
Figure 8 : Streamlines over a protruding heater on the plane *yz for x*= 2,375*H*

In Figure 9, the laminar flow streamlines around a 3D protruding heater are presented in the plane xy for different positions of z considering Re = 200.

(a) z = 0

(b) z = 0,08H

(c) z = 0,16H

(d) z = 0,24H

(e) z = 0,32H
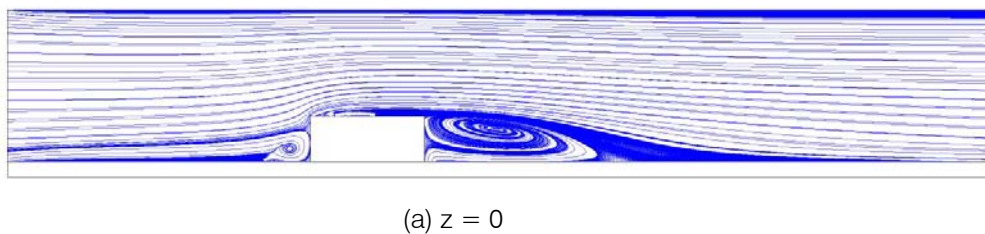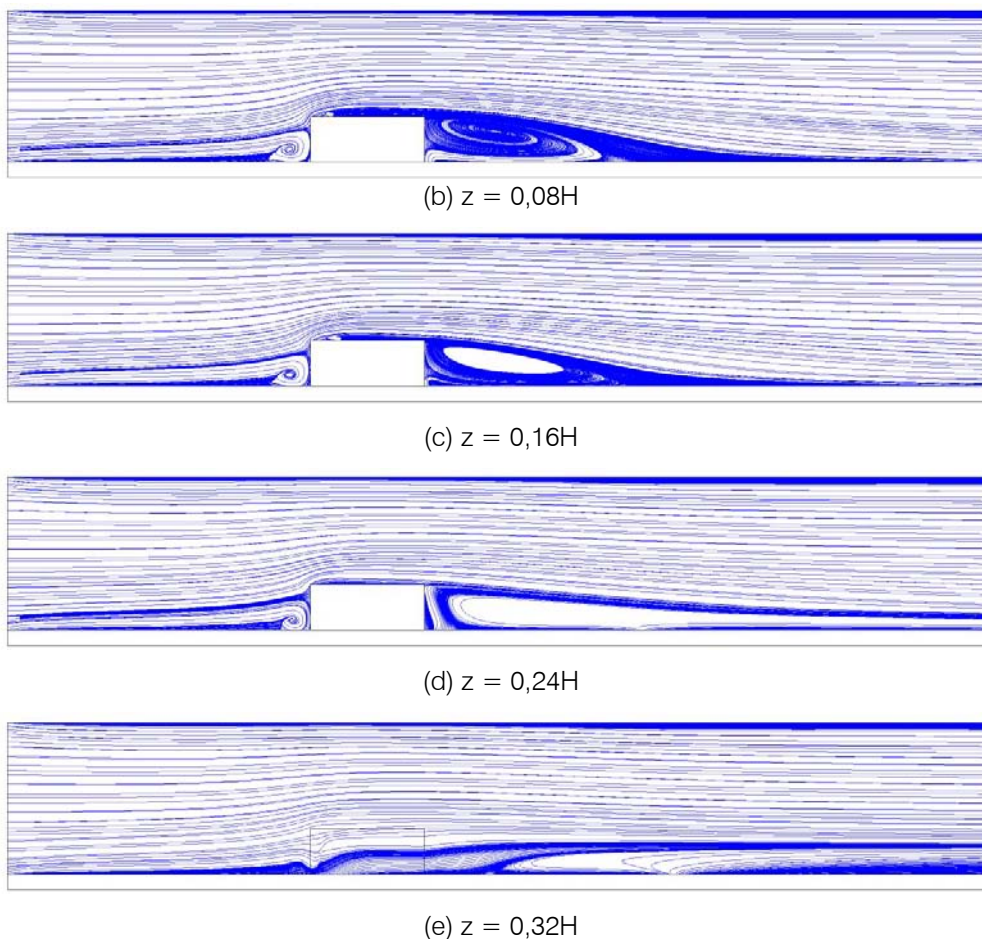
Figure 9 : Streamlines over a protruding heater on the plane **xy** considering *Re* = 200

In Figure 10, the laminar flow streamlines around a 3D protruding heater are presented in a plane *xz* for different positions of *y*, considering *Re* = 200.

(a) y = 0,16H

(b) y = 0,24H

(c) y = 0,32H

(d) y = 0,40H

(e) y = 0,44H
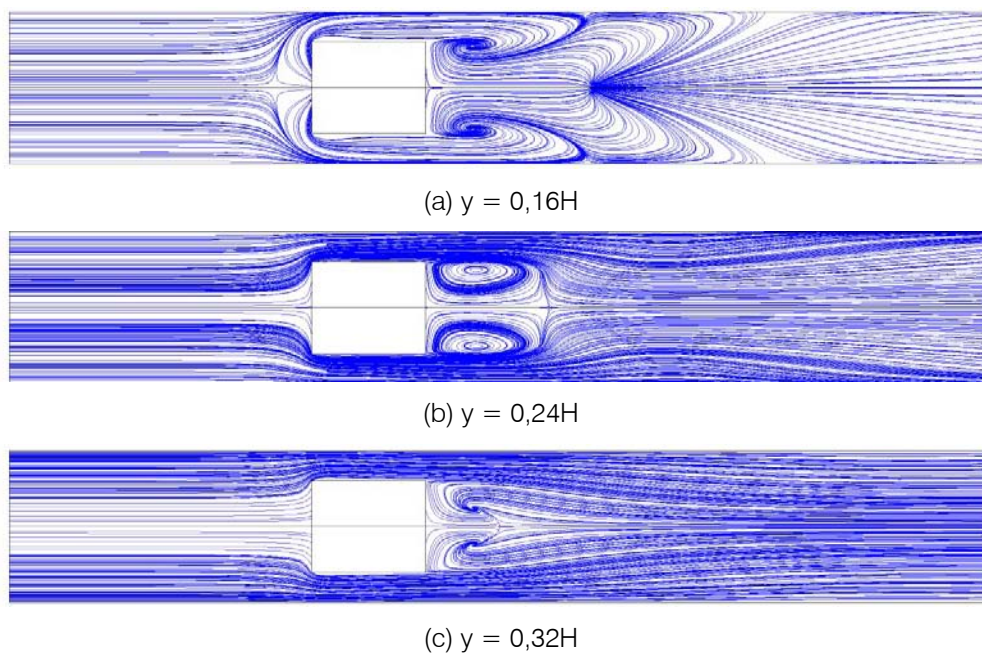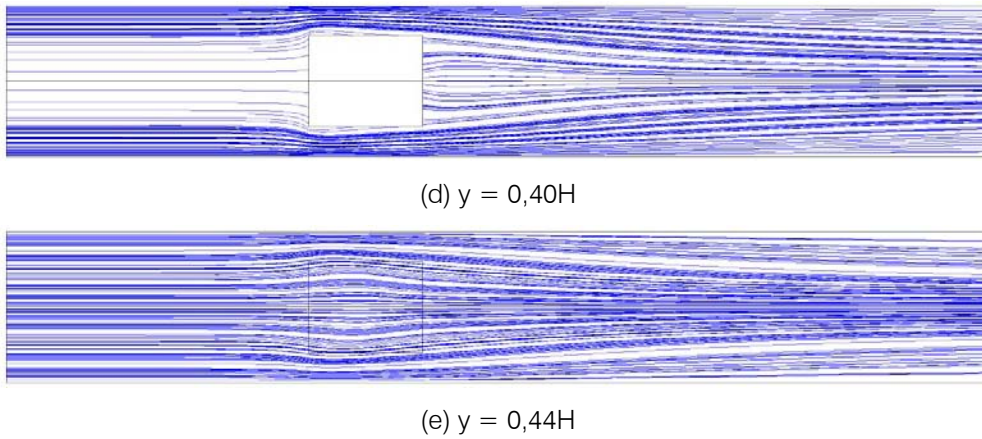
Figure 10 : Streamlines over a protruding heater on the plane *xz* considering *Re* = 200

The recirculation length (L_{rec}) downstream the protruding heater, or the distance between the base of the heater's rear surface and the reattachment point of the fluid's boundary layer, is presented in function of *Reynolds* in Tab. 1. The same results are shown in Fig. 11, where it is observed that the recirculation length varies linearly with *Re*. A correlation with deviations smaller than 0.35% is presented in Eq. (7). From all presented results, the greatest length (L_{rec}) was approximately 2.75*H*, ensuring that the recirculation is always in the studied domain.

Table 1 : Length Lrec of the recirculation downstream the protruding heater

Re	L_{rec}/H
100	1.19
150	1.60
200	2.00
250	2.43
300	2.84

$$(L_{rec}/H) = 0.0083\,Re + 0.3602, \qquad (7)$$
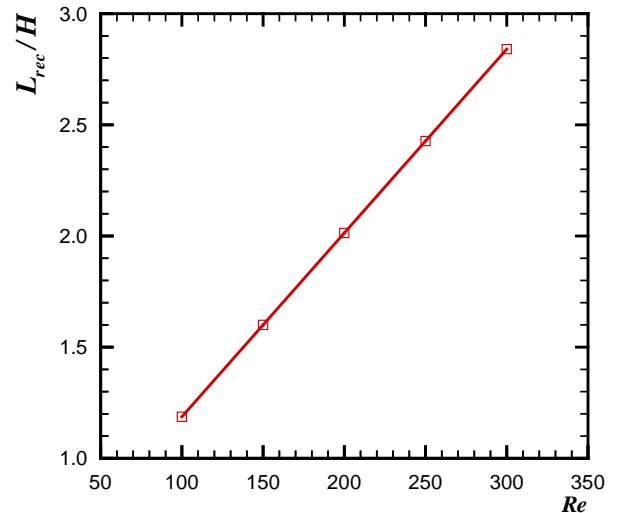
Figure 11 : Length L_{rec} of the recirculation downstream the protruding heater

In Figures 12, 13, and 14 the air laminar flow velocity profiles are presented for the planes *xy*, *xz* e *yz*, respectively. The same fluid dynamic behavior is observed when compared with Figs. 6, 7, and 8.

(a) Re = 100

(b) Re = 200

(c) Re = 300

0.000   0.257   0.515   0.772   1.030

Velocity   [m s^-1]

0   0.03   0.060 (m)
    0.015   0.045
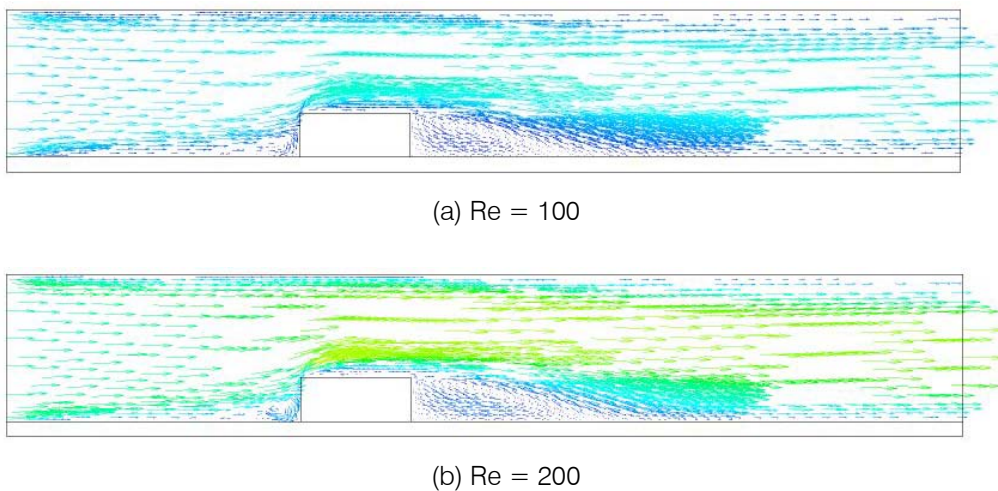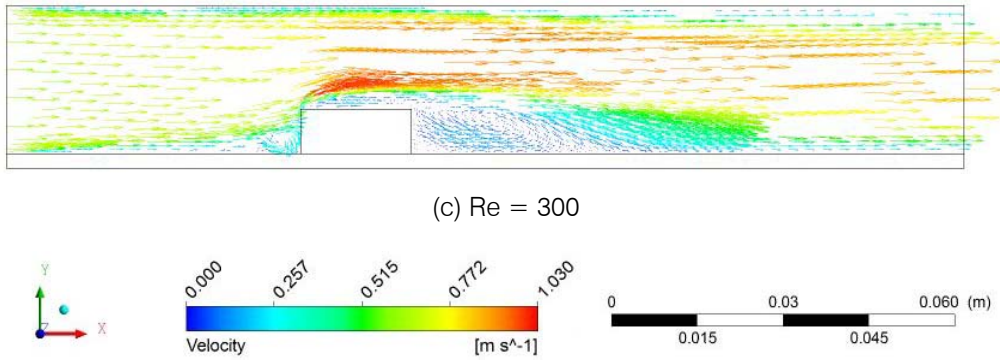
Figure 12 : Air velocity profile over a protruding heater on the plane xy for z = 0

(a) Re = 100

(b) Re = 200

(c) Re = 300

0.000   0.257   0.515   0.772   1.030

Velocity   [m s^-1]

0   0.025   0.050 (m)
    0.0125   0.0375
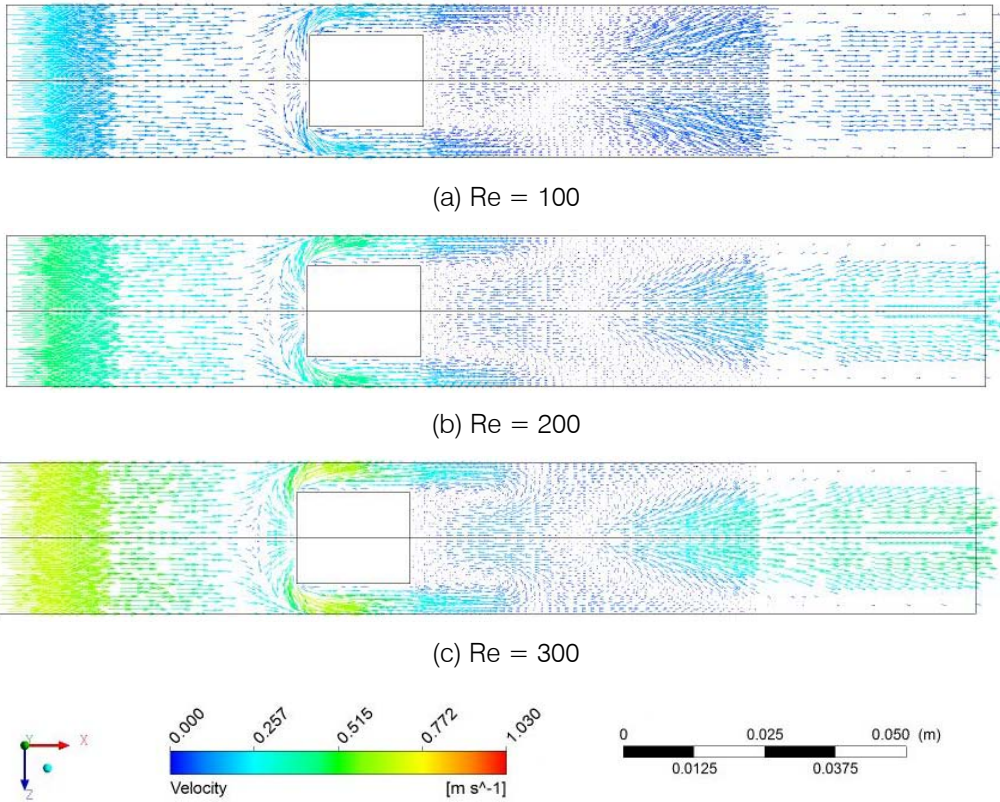
Figure 13 : Air velocity profile over a protruding heater on the plane *xz* for *y* = 0,16*H*

(a) Re = 100

(a) Re = 200

(a) Re = 300
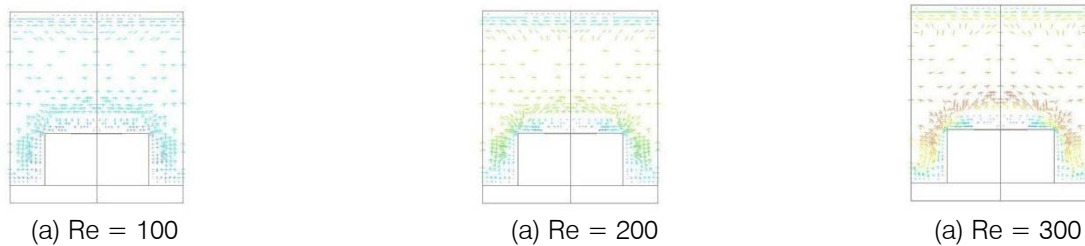
Figure 14 : Air velocity profile over a protruding heater on the plane *xz* for *y*= 2,375*H*

The air velocity profiles along the *y* direction of two positions upstream the heater and four positions downstream the heater are shown in Figs. 15(a) e 15(b), respectively, considering *Re* = 200. The recirculations' behavior can be better observed from the *x* direction velocity component values. A negative velocity value (*u*) represents a reverse flux in relation to the main flow.

(a) Region upstream the heater

(b) Region downstream the heater
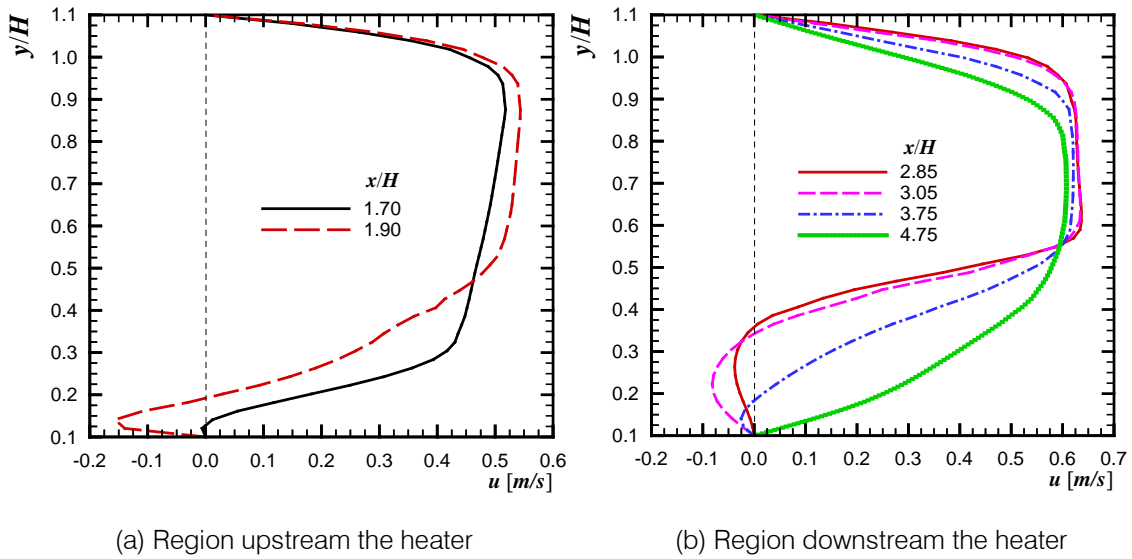
Figure 15 : Air velocity profile along the y direction for different positions for *Re* = 200

In Figures 16, 17, and 18 are presented pressure distributions of the air laminar flow for the planes *xy*, *xz* e *yz*, respectively. As expected, the region upstream the protruding heater has a greater pressure than the downstream region. Independently of the *Reynolds* number, the largest pressures found are around the 3D heater's front surface due to the stagnation point. Furthermore, the larger the *Re*, the larger the pressure gradients are close to the stagnation.

(a) Re = 100

(b) Re = 200

(c) Re = 300
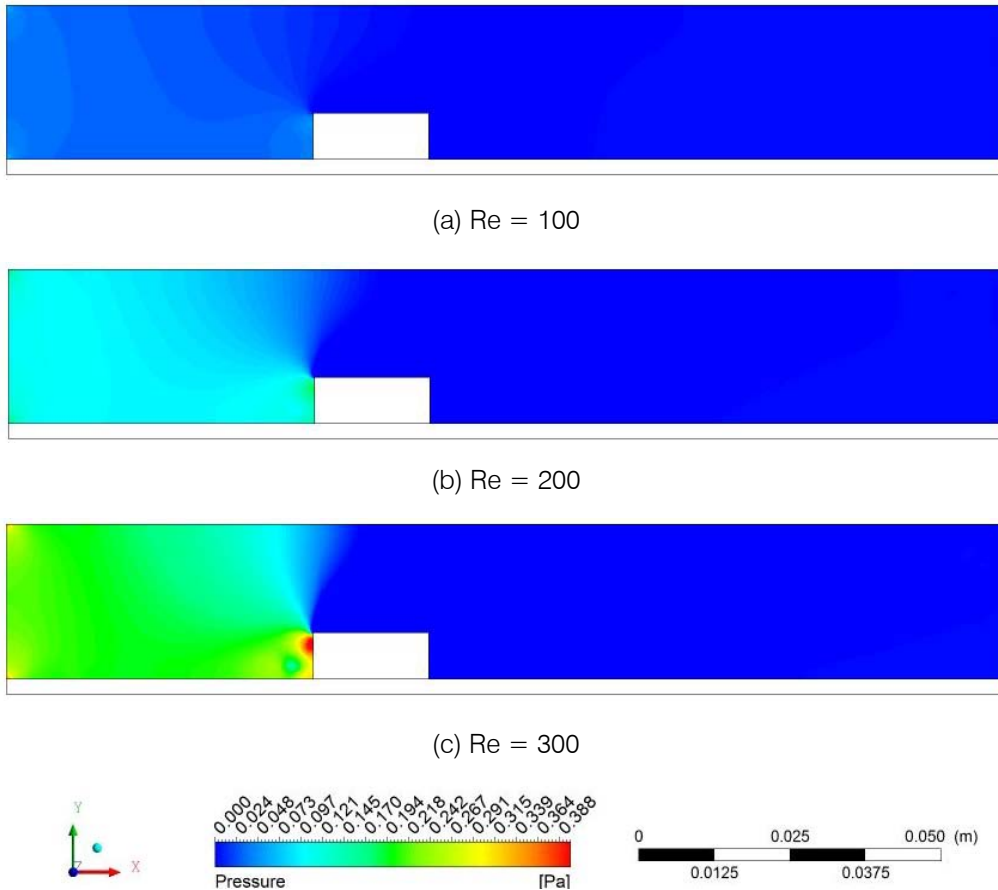
Figure 16 : Air pressure distribution map on the *xy* plane for *z* = 0

(a) Re = 100

(b) Re = 200

(c) Re = 300
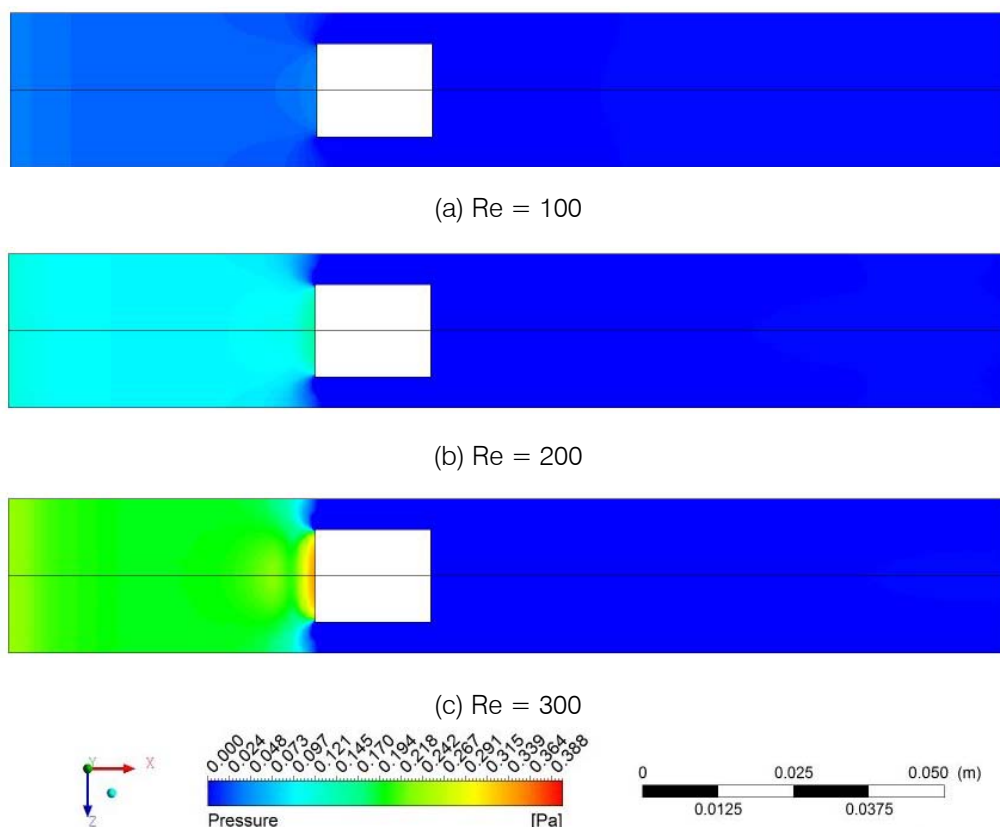
Figure 17 : Air pressure distribution map on the *xy*plane for*z* = 0,16H

(a) Re = 100

(a) Re = 200

(a) Re = 300
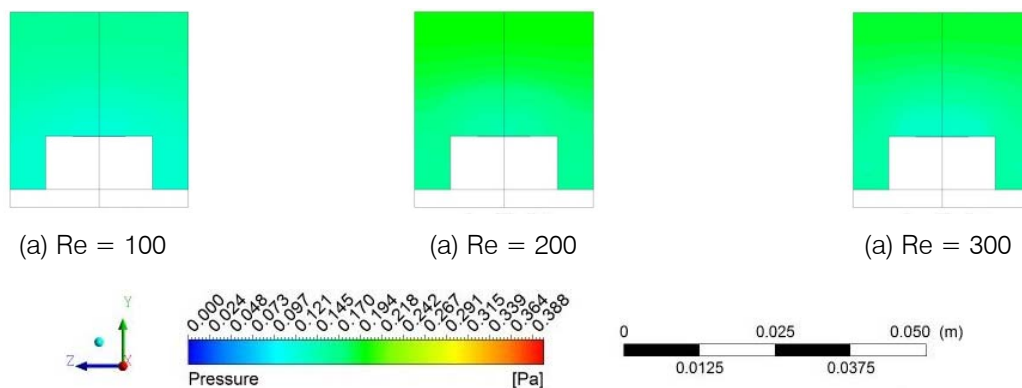
Figure 18 : Air pressure distribution map on the *xy*plane for*z* = 2,375H

In order to assist the identification of the lines of interest on the different faces of the 3D protruding heater, notation presented in Fig. 19 is used in this work.

(a) line ABCD

(b) line EFGH

(c) line IJKL
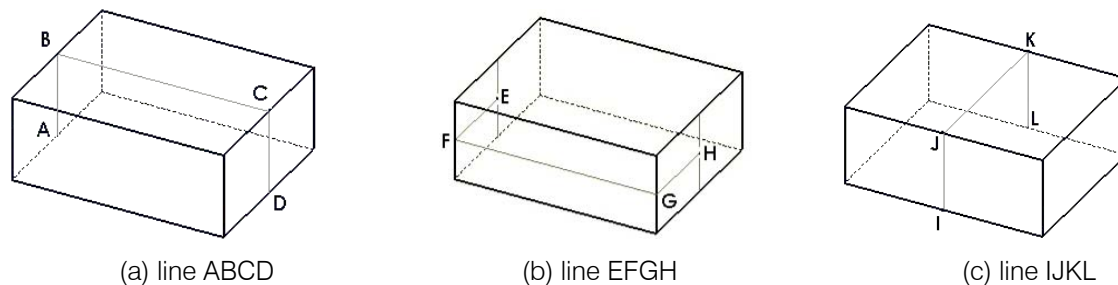
Figure 19 : Identification of the lines of interest on the faces of a 3D protruding heater

33

Figure 20 shows the local skin friction coefficient distribution along the central line of the channel's superior wall (x; 1,1H; 0) in function of the *Reynolds* number. The behavior of $C_{f,x}$ in function of x can be observed. It is noticed that $C_{f,x}$ dramatically falls in the parallel plate channel's inlet, it lightly increases in the region close to the protruding heater, decreases in the region downstream the heater, and remains constant after approximately $x = 4,5H$ for all *Reynolds* values.
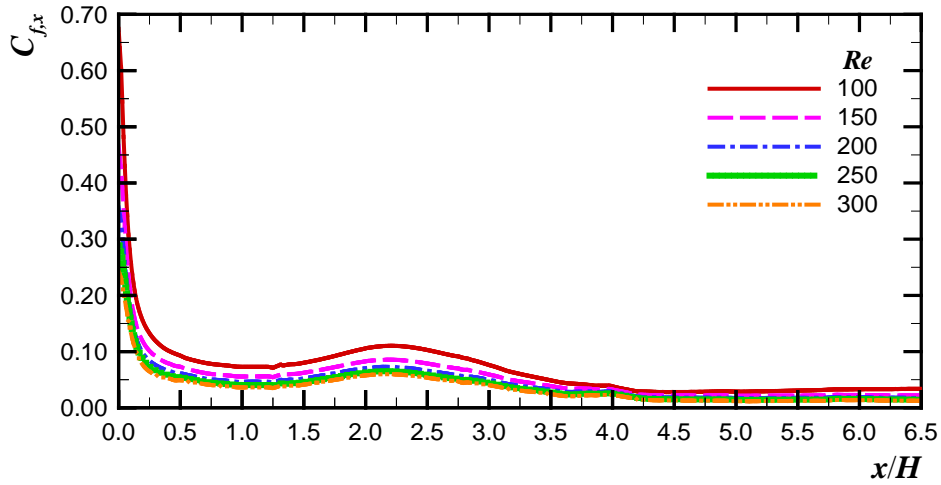
Figure 20 : Local skin friction coefficient distribution along the central line of the channel's superior wall

Figure 21 presents the local skin friction coefficient distribution along the length of the central line of the channel's bottom wall in a region upstream the 3D protruding heater (1,2$H \leq x \leq$ 2,0H; 0,1H; 0) in function of *Reynolds*. From the behavior of $C_{f,x}$ in function of x for lower *Re* numbers, such as, $Re = 100$ and 150, it appears that only one horseshoe vortices is formed, however two horseshoe vortices are formed for higher *Reynolds* numbers, $Re = 200$, 250, and 300.
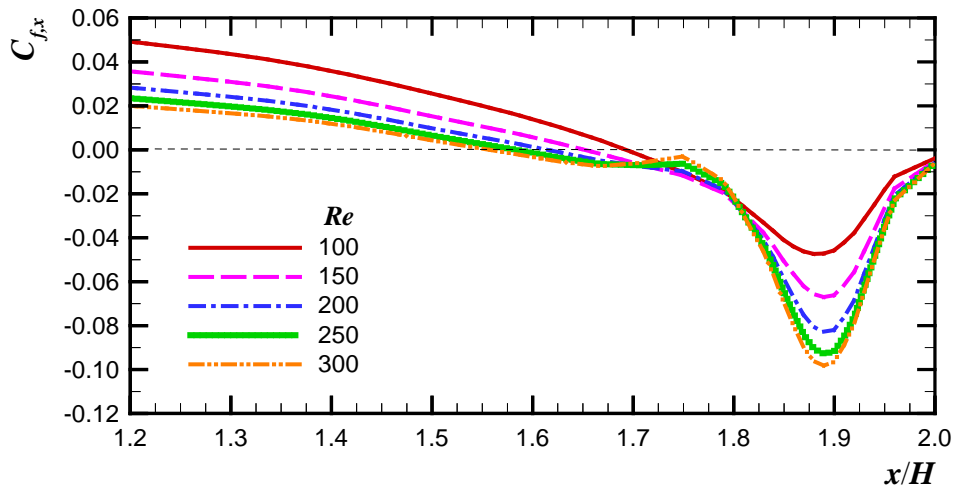
Figure 21 : Local skin friction coefficient distribution along the central line of the channel's bottom wall, in a region upstream the protruding heater

Figures 22(a), 22(b) e 22(c) ilustrate the variations of the friction coefficient along the lines ABCD, EFGH e IJKL, respectively, on the 3D protruding heaters' surfaces. It is observed that in Figure 22(a) on the front surface of the heater, $C_{f,y}$ is negative, showing that there is a flow from the central region (stagnation point) to the side of the protruding heater. On the superior (top) surface of the heater, there is a region of negative values of $C_{f,x}$, except for $Re = 100$, representing the fluid's boundary layer separation, and the region of flow recirculation (reverse flux) in the clockwise direction. On the rear surface of the heater, $C_{f,y}$ is positive, indicating that the recirculation downstream the protruding heater occurs in the

clockwise direction. The laminar flow characteristics along the lines EFGH e IJKL on the surfaces of a 3D protruding heater can be explained in a similar way trough the analysis of Figs. 22(b) e 22(c), respectively.
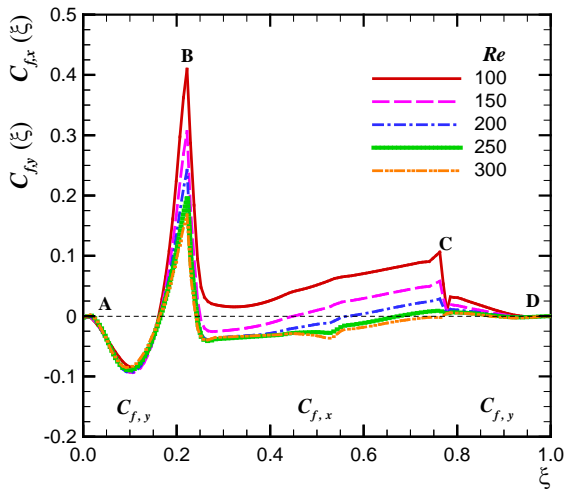
(a) line ABCD
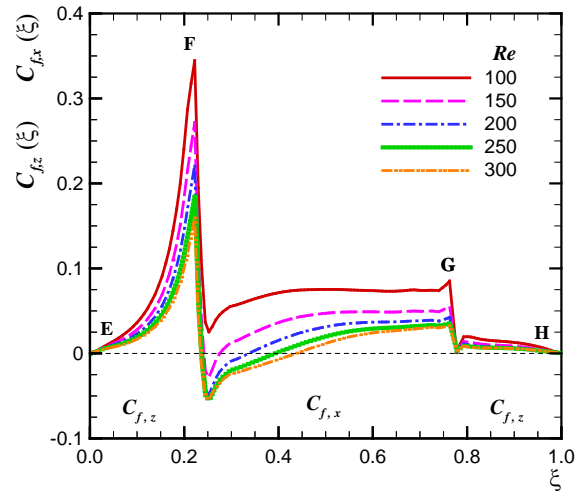
(b) line EFGH
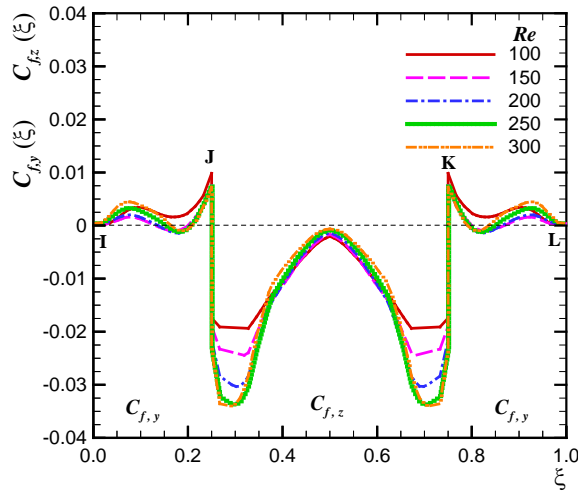
(c) line IJKL

Figure 22 : Local skin friction coefficient distribution

The results for the *Darcy-Weisbach*(or *Moody*) friction factor and the mean friction coefficient can be correlated with deviations smaller than 1.5% using

$$\overline{C}_f = 0,051\, Re^{-0,359}, \qquad (8)$$

$$f = 0,204\, Re^{-0,359}. \qquad (9)$$

Figures 23 and 24 illustrate the behavior of the mean friction coefficient and the *Darcy-Weisbach*(or *Moody*) friction factor, respectively, in function of the *Reynolds* number. As expected, these fluid-dynamic parameters decrease with the increasing *Re*.
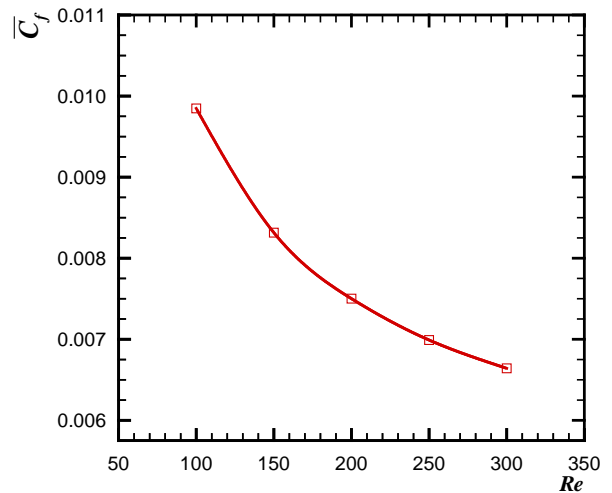
Figure 23 : Mean friction coefficient in function of the *Reynolds* number
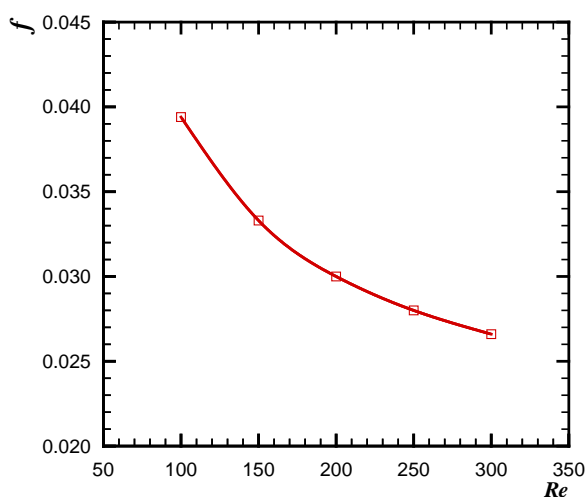
Figure 24 : Darcy-Weisbach (*or Moody*) friction factor in function of the Reynolds number

IV. Conclusions

In this work, a numerical analysis of the laminar flow around an array of 3D protruding heaters mounted on the bottom wall (substrate) of a parallel plate channel was made utilizing the commercial software *ANSYS/Fluent*® 14.0. Air was considered as the cooling fluid. The cooling process occurred through a forced laminar flow with constant properties under steady state conditions. At the channel's inlet, the velocity profile of the flow was uniform. The conservation equations and the respective boundary conditions were numerically solved in a single domain that incorporated the regions of solid and fluid, through a coupled procedure utilizing the Control Volume Method. The occasional effects of oscillation in the flow were not considered. Due to the problem symmetries, the basic configuration of the problem was reduced to the one in Fig. 2 and the solution domain utilized was showed in Fig. 3. Typical geometry and property values, relevant to the electronic components mounted on printed circuit board cooling applications, were used to obtain the numerical results. The geometric configuration showed in Fig. 2, were assumed considering a space $H = 0.0254$m between the parallel plates. The effects of the *Reynolds* number, based on the protruding heaters height, were inspected for $Re = 100, 150, 200, 250,$ and 300. The flow in the channel was always laminar for the range of *Re* investigated.

The behavior of the laminar flow over the 3D protruding heaters mounted in cross-stream direction was showed through the streamlines. The streamlines over a 3D protruding heater were presented for *Reynolds* numbers of 100, 200, and 300. The main characteristics of the laminar flow were the horseshoe vortices which start upstream the heater and develop around the heater's lateral surfaces; a small recirculation upstream the protruding heater; the fluid's boundary layer detachment at the top of the heater causing a recirculation (reverse flux); and a large recirculation region downstream the heater due to the flow reattachment. The recirculation length (L_{rec}) downstream the protruding heater varies linearly with *Re*. The velocity magtintudes, the recirculation directions and the pressure distributions at the different regions of the air laminar flow, were presented for the planes *xy*, *xz* e *yz*. The local skin friction distribution on the walls of the parallel plate channel and on the 3D protruding heater surfaces, were also showed.

It is interesting to state that the fluid flow development around the 3D protruding heaters lateral surfaces does not freely happen due to the small space between the heaters. The fluid-dynamic symmetry conditions of the blocks were dominant and the corresponding flow was different than a single 3D protruding heater with free domain in the cross-stream direction to the flow.

V. Acknowledgements

References Références Referencias

1. J.Y. Hwang & K.S. Yang, "Numerical study of vortical structures around a wall-mounted cubic obstacle in channel flow", *Phy.Fluids*Vol. **16**, pp. 402-020, (2004).
2. A. Van Dijk& H.C. De Lange, "Compressible laminar flow around a wall-mounted cubic obstacle", *Comp. Fluids* Vol. 36, pp. 949-960, (2007).
3. I.P. Castro & A.G. Robins, "The flow around a surface-mounted cube in uniform and turbulent streams", *J. Fluid Mech.* Vol. **79**, pp. 307–335, (1977).
4. R.J. Martinuzzi& C. Tropea "The flow around surface mounted prismatic obstacle placed in fully developed channel flow", *J. Fluids Eng.* Vol. **115**, pp. 85–92, (1993).
5. C.D. Tropea& R. Gackstatter, "The flow over two-dimensional surface-mounted obstacles at low Reynolds numbers", *J. Fluids Eng.* Vol. **107**, pp. 489–494, (1985).
6. S. Okamoto, T. Katsumata, N. Abe & M. Kijima, "Flow past repeated ribs of a square section mounted on a ground plate", *Trans. Jpn. Soc. Mech. Eng.* Vol. **63B**, pp. 3834–3842, (1997).
7. T.A. Alves, *Resfriamento conjugado de aquecedoresdiscretosemcanais.*Tese (DoutoradoemEngenhariaMecânica) – Faculdade de EngenhariaMecânica, UniversidadeEstadual de Campinas, Campinas, (2010).
8. T.A. Alves& C.A.C. Altemani, "An invariant descriptor for heaters temperature prediction in conjugate cooling", *Int. J. Thr. Sci.* Vol. **58**, pp. 92–101, (2012).

9. J. Davalath& Y. Bayazitoglu, "Forced convection cooling across rectangular blocks", *J. Heat Tr.,* Vol. **109**, pp. 321–328, (1987).

10. Y. Zeng & K. Vafai, "An investigation of convective cooling of an array of channel-mounted obstacles", *Num. Heat Tr., Part A,* Vol. **55**, pp. 967–982, (2009).

11. S.V. Patankar, *Numerical heat transfer and fluid flow.* Hemisphere Publishing Corporation, (1980).

12. A. Bar-Cohen, A.A. Watwe& R.S. Prasher, *Heat transfer in electronic equipment.* In: A. Bejan& A.D. Kraus (Eds.) *Heat transfer handbook.* John Wiley & Sons, (2003). Chap.**13**, pp.947-1027.

13. F.P. Incropera, D.P. Dewitt, T.L. Bergman & A.S. Lavine, *Fundamentos de transferência de calor e de massa.*LivrosTécnicos e CientíficosEditora, (2008).

14. G.K. Morris & S.V. Garimella, "Thermal wake downstream of a three-dimensional obstacle". *Exp. Th. Fluid Sc.,* Vol. **12**, pp. 65-74, (1996).

15. F.B. Nishida, *Análisenumérica do escoamento laminar e da transferência de calor de aquecedores 3D protuberantesmontadosemumaplaca de circuitoimpressoutilizandodiferentesfluidos de resfriamento.* Monografia (Trabalho de Conclusão de Curso de Graduação) – UniversidadeTecnológica Federal do Paraná, Ponta Grossa, (2012).

This page is intentionally left blank

38